Supplementary methods

Mechanistic model

Here we use a deterministic version of a well-established and highly utilised compartmental model of *Plasmodium falciparum* malaria transmission (1-5), which models transmission within humans and vectors at various stages of infection. We account for heterogeneity in transmission as well as age-dependent biting rates and the acquisition of natural immunity. The model has previously been described fully in the aforementioned publications, but we summarise it briefly below (Appendix Figure **1**).

When Susceptible (S) individuals become infected, they progress to either an asymptomatic (A) state or clinical disease, at a rate dependent on the force of infection, Λ, and the probability of acquiring clinical disease, φ, which is itself dependent on natural immunity. Those progressing to clinical disease either enter the treated (T) or clinical disease (D) compartment dependent on the probability of treatment (f_T). Treated individuals progress through to a period of protection through prophylaxis (P), at rate r_T, and return to the susceptible compartment at rate r_P.

Individuals in clinical disease (D) remain symptomatic for the duration of the disease course, r_D, then move to an asymptomatic state (A), which is detectable through microscopy, before the infection becomes submicroscopic (so undetectable through microscopy, U) at rate r_A. Asymptomatic individuals (in either the A or U compartment) can develop clinical disease, but if they do not, they clear the infection and return to the symptomatic compartment at rate r_U. Adult mosquito populations are modelled through a susceptible (S_m) and progress to the exposed (E_m) state at rate Λ_m, and onto the infectious (I_m) after the extrinsic incubation period (EIP) has been completed. Mosquitoes are exposed to human infection through feeding through the treated (T), clinical disease (D), asymptomatic (A) and submicroscopic (U) infection states.

Vector control interventions are assumed to reduce malaria by primarily killing adult mosquitoes but also through dissuading them from biting. The use of insecticide treated nets (ITNs) is incorporated in the model structure using the methods outlined in Le Menache et al., 2007(6) and Griffin et al. 2010(3). Entomological data has shown that ITNs are less effective against pyrethroid resistant mosquitoes (as described by the percentage of mosquitoes surviving a discriminating dose bioassay). The efficacy of ITNs in Ethiopia is calculated using local discriminating dose bioassay data and methods outlined by Churcher *et al* (2016)(7). The efficacy of indoor residual spraying (IRS) was parameterised using Sherrard-Smith et al 2018 whilst larval source management was assumed to reduce mosquito emergency by a defined value.

Models were parameterised for each site individually taking into account the history of control interventions (see main text for a description and Figure A2 for values). The human-to-mosquito ratio was varied to match the observed malaria prevalence in the defined cohort. To simulate the invasion of *Anopheles stephensi*, the vector density is increased in a

sigmoidal fashion over 3 years to approximately match the patterns seen in malaria incidence in Djibouti.

The package required to run the model and a version of the model code is found at https://github.com/mrc-ide/deterministic-malaria-model.

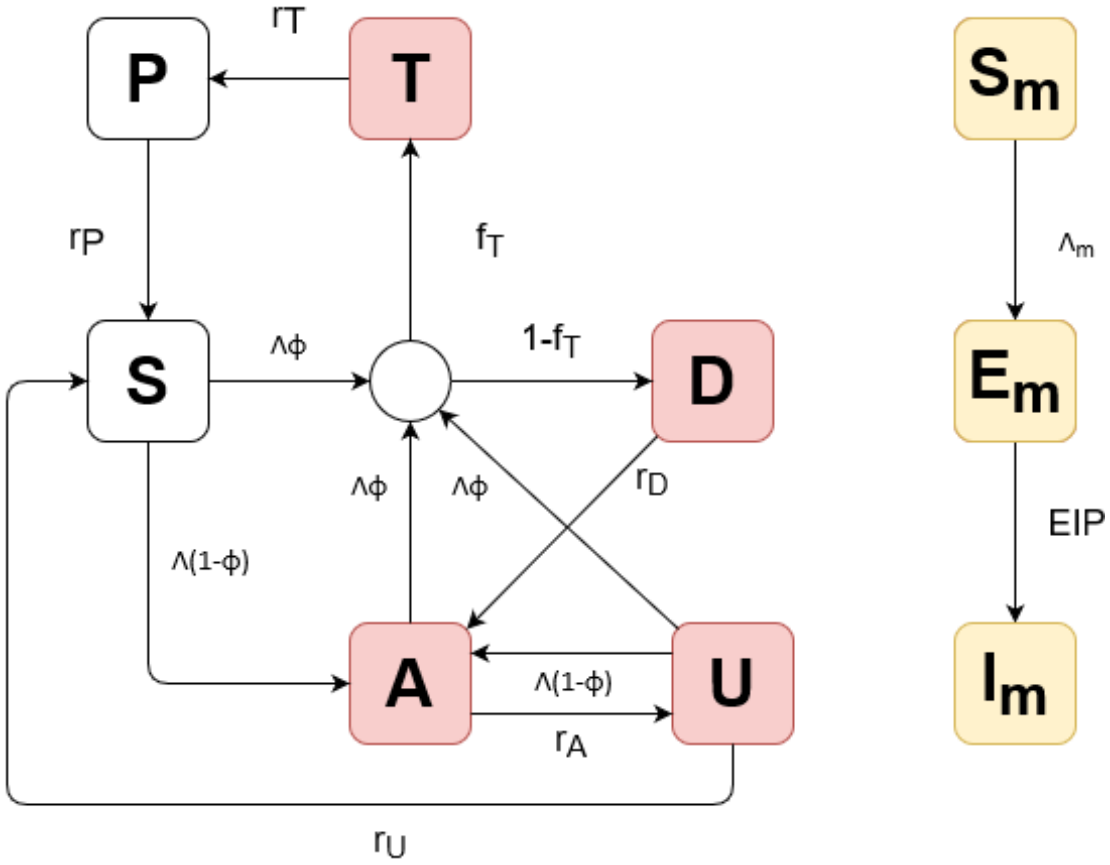

Appendix Figure 1. Model diagram showing the progression between human and vector states. Humans are either S = susceptible, A = asymptomatic, T = treated, D = have clinical disease, or U = submicroscopic infection, whereas mosquitoes are either S_m = Susceptible, E_m = infected but not infectious, I_m = infectious. The arrows shown transitions between compartments and the circle represents treatment. Red compartments indicate states that can expose susceptible mosquitoes to infection and yellow the mosquito compartments. The life-cycle of the pre-adult life-stages of the mosquito are omitted for simplicity though see (4) for full details.

Human population sizes and pre-existing malaria prevalence

Administrative unit human population sizes were obtained by using WorldPop 2020 population raster, which provides population estimates at a 1/120 degree resolution (8). This was then standardised to the 2020 Ethiopia country level population estimate from the UN World Population prospects (9). This raster was then applied to the administrative boundaries in order to estimate populations in each unit.

To estimate the population below a certain altitude or within areas found suitable by previous research (10), we applied theses limits to the above standardised population raster using a

suitability raster provided by Sinka et al., (2020) and altitude from WorldClim (11). Malaria prevalence, *P. falciparum*, in 2-10-year olds is provided by the Malaria Atlas Project (MAP) and aggregated to the administrative level by taking the population weighted mean.

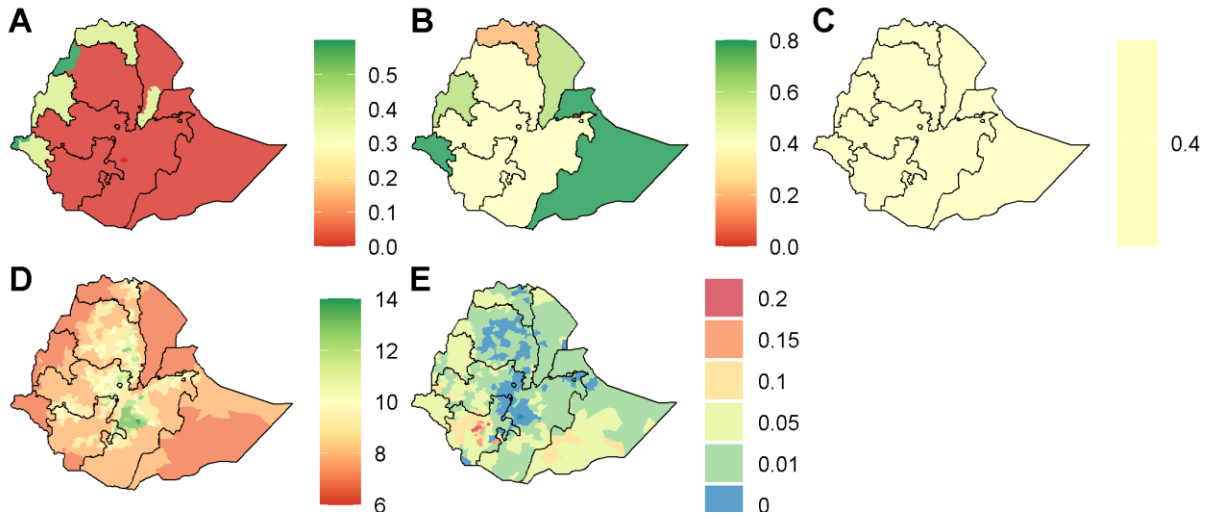

Appendix Figure 2. Parameters included for each administrative grouping. A) IRS coverage (%), B) ITN coverage (%), C) treatment coverage (%), D) extrinsic incubation period (days), E) Prevalence in 2-10-year-olds.

Temperature and EIP estimates

Temperature data was accessed by WorldClim (11) which provided monthly temperature data at the maximum, mean and minimum for 2010-2018.

Highland regions of Ethiopia are predicted to be too cold to sustain malaria transmission throughout the year. As a result, here we have used the hottest months mean maximum temperature in the year, as it represents the "extreme" scenario – with the fastest EIP. While this may overestimate the value of EIP overall, the majority of malaria transmission occurs in relatively short "transmission seasons", and so it only takes a few months of heightened suitability in an otherwise less suitable temperature clime to have a substantial effect. This was then averaged over the period to produce a single raster file of temperature at a resolution of 1/120 degrees.

This temperature was then converted into EIP estimates based on a previous quantification by Stopard et al., (2021) which provided a description of the temperature dependent relationship of *P. falciparum* in *An. stephensi* (12) (Appendix Figure **3**). These estimates were derived in laboratory populations of mosquitoes and parasites though is assumed to hold for wild *An. stephensi* mosquitoes infected with *P. falciparum* in Ethiopia (13-16). For simplicity it is assumed that all mosquitoes have the same EIP. As this temperature relationship was modelled on a limited set of temperatures (21-34 °C) it was necessary to extrapolate this further to capture the temperature range of Ethiopia. This EIP estimate was converted to the administrative level by taking the mean EIP in an area (Appendix Figure **2D**). All other

mosquito bionomics and factors influencing transmission biology are assumed to be independent of temperature or altitude.

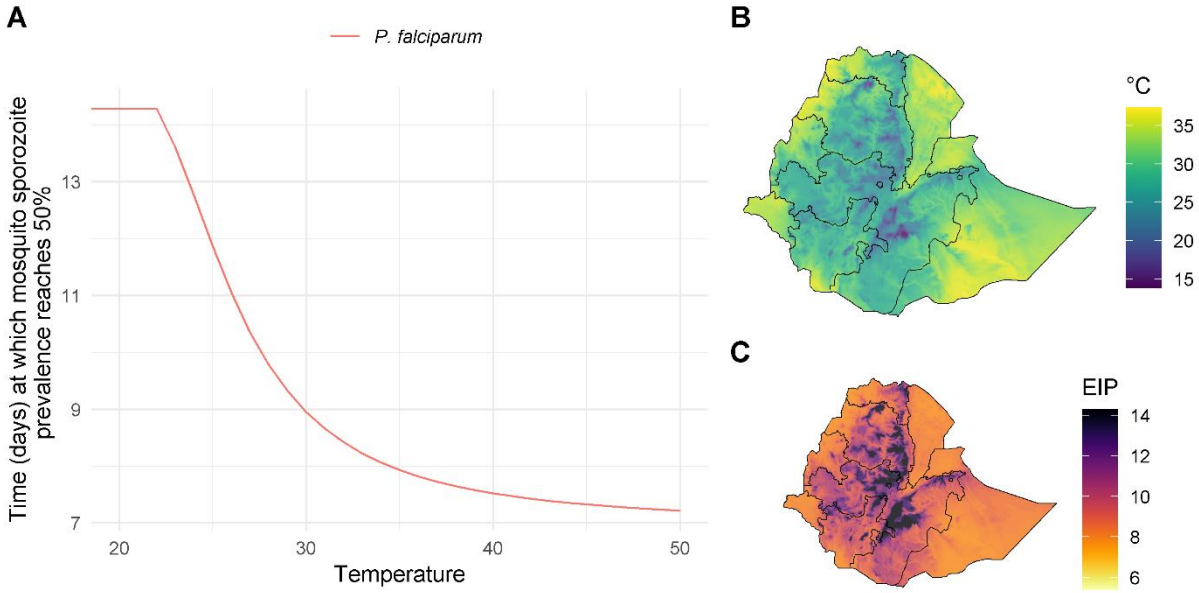

Appendix Figure 3. How parasite extrinsic incubation period is assumed to vary across Ethiopia. A) Relationship between the extrinsic incubation period and temperature for the development of *Plasmodium falciparum* in *Anopheles stephensi* in laboratory studies. B) The maximum monthly annual temperature across Ethiopia. C) Predicted EIP (days) derived from the maximum temperature for *P. falciparum.*

Mosquito bionomics

The results of a literature search for the key mosquito bionomics parameters are summarised in Appendix Table 2. Data re relatively scant and those studies that were identified show *An. stephensi* estimates vary substantially in its native range. In addition, very few studies were identified within the context of Djibouti or Ethiopia. To account for this uncertainty a wide range of parameter distributions were used which are presented in (Appendix Figure **4**A).

Shapefiles and grouping administrative units

Shapefiles were provided through the humanitarian data exchange (https://data.humdata.org/dataset/ethiopia-cod-ab) at the country, 1st, 2nd and 3rd administrative unit level. Administrative units at the 3rd level were grouped based on their pre-existing transmission, interventions and EIP. Here we round prevalence to the nearest 5%, with an additional value of 1% as to capture areas with low but not negligible levels of transmission which account for much of Ethiopia. Interventions and treatment coverages were rounded to the nearest 20% and EIP to the nearest integer. This rounding allows us to substantially reduce the number of runs required, and by using approximate rather than "exact" values from the data we aim to not overstate the accuracy of our findings. By then grouping administrative locations by their combination of parameters, we can reduce the

number of simulations required for each model run from 690 (each individual adm3 location) to 64. Full details of the diversity of groups are shown in Appendix Table 1.

Table 1. Mosquito parameters and values used in Latin hypercube sampling.

Parameter	*Values*
Daily mortality	0.093 – 0.154
Proportion of blood meals taken on humans, anthropophagy	0.1 – 0.4
Proportion of mosquitoes resting inside, endophily	0.375 – 0.625
Proportion of mosquito bites taken when people indoors (in absence of interventions)	0.358 – 0.597
Proportion of mosquito bites taken when people in bed (in absence of control interventions)	0.391 – 0.652

Appendix Table 2. Grouping of administrative units and the number of admin units per category (total 650), by *P. falciparum* prevalence (%), IRS/ITN coverage (%) and EIP (days).

ID	*No. admin units*	*P. falciparum prevalence (2-10 years)*	*IRS*	*ITN*	*EIP*
1	1	0	0%	40%	14
2	11	0	0%	40%	13
3	2	0	0%	0%	12
4	22	0	0%	40%	12
5	4	0	0%	0%	11
6	28	0	0%	40%	11
7	1	0	40%	20%	10
8	26	0	0%	40%	10
9	3	0	40%	20%	9
10	31	0	0%	40%	9
11	1	0	40%	20%	8
12	15	0	0%	40%	8
13	1	0	0%	80%	8
14	1	0	0%	40%	7
15	3	0	0%	60%	7
16	2	0.01	0%	40%	13
17	3	0.01	0%	40%	12
18	11	0.01	0%	40%	11
19	3	0.01	40%	20%	10
20	50	0.01	0%	40%	10
21	5	0.01	40%	20%	9

22	68	0.01	0%	40%	9
23	2	0.01	0%	80%	9
24	2	0.01	0%	0%	8
25	11	0.01	40%	20%	8
26	117	0.01	0%	40%	8
27	3	0.01	40%	60%	8
28	13	0.01	0%	80%	8
29	3	0.01	40%	20%	7
30	4	0.01	0%	40%	7
31	2	0.01	60%	40%	7
32	19	0.01	0%	60%	7
33	1	0.01	20%	60%	7
34	8	0.01	40%	60%	7
35	12	0.01	0%	80%	7
36	6	0.05	0%	40%	11
37	2	0.05	0%	40%	10
38	1	0.05	40%	20%	9
39	28	0.05	0%	40%	9
40	1	0.05	40%	20%	8
41	59	0.05	0%	40%	8
42	2	0.05	0%	60%	8
43	6	0.05	40%	60%	8
44	4	0.05	0%	80%	8
45	2	0.05	20%	80%	8
46	5	0.05	40%	20%	7
47	3	0.05	0%	40%	7
48	1	0.05	60%	40%	7
49	2	0.05	0%	60%	7
50	8	0.05	40%	60%	7
51	16	0.05	0%	80%	7
52	7	0.05	40%	80%	7
53	4	0.05	60%	80%	7
54	1	0.1	0%	40%	11
55	2	0.1	0%	40%	10
56	6	0.1	0%	40%	9
57	21	0.1	0%	40%	8
58	1	0.1	0%	80%	8
59	1	0.1	0%	40%	7
60	4	0.1	0%	80%	7
61	1	0.15	0%	40%	10
62	1	0.15	0%	40%	9
63	4	0.15	0%	40%	8
64	2	0.2	0%	40%	8

Cost of interventions per person

Approximate estimates of the cost of intervention (purchasing, delivering, and applying) were provided from literature and from the PMI through personal communication. We have assumed 1.8 people per ITN, which were assumed to be standard pyrethroid nets.

Appendix Table 3. Approximate estimated costs per person per year for the different vector control interventions considered.

Intervention	*Costing estimate per year per person*		
	Low	Medium	High
ITN-PBO-pyrethroid	$0.56	$0.61	$0.66
ITN-pyrethroid	$0.43	$0.45	$0.49
IRS	$3.35	$6.19	$8.9
Larvicide	$1.00	$2.00	$3.00

Supplementary results

Model fit to Djibouti data

A hundred models varying mosquito bionomics were fit to the MAP estimates of annual clinical incidence in Djibouti (Appendix Figure 4B). Anthropophagy refers to the proportion of blood meals taken on humans, endophagy bed refers to the proportion of blood meals taken in bed, endophagy indoors the proportion of blood meals taken indoors, endophily the proportion of time spent around human houses and mortality, the daily probability of an adult mosquito dying. Overall, there was a very high rate of agreement between the model estimates and the data, with point estimates approximately equally and well within 95% CI's.

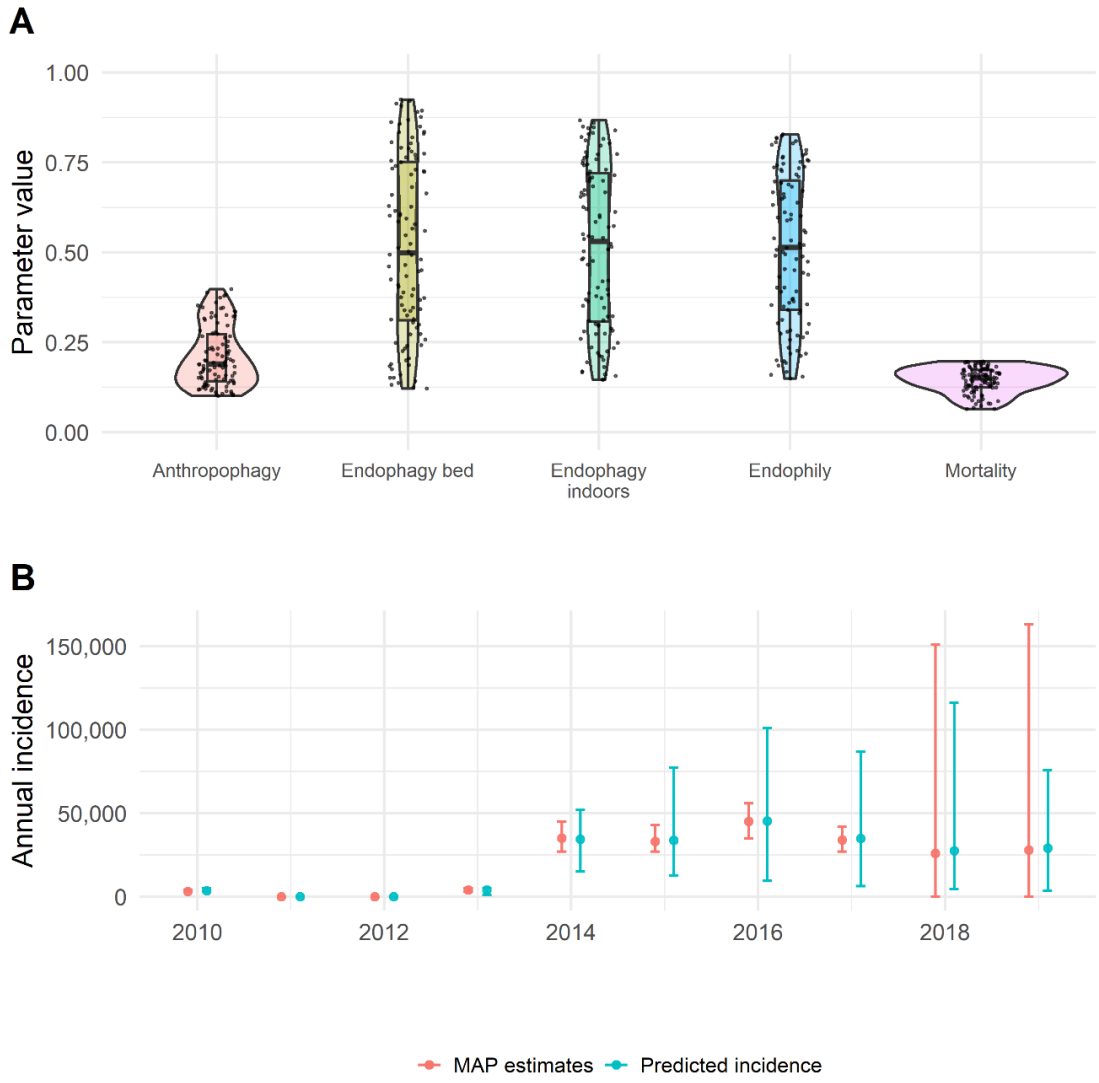

Appendix Figure 4. Vector bionomics parameter distributions and fitted model incidence compared to the MAP estimates calibrated against. A) The distribution of the parameters used from the 100 best LHC models. Violin plots show density of data, the boxplot the quantiles and outliers and the points the individual values. B) The model predicted incidence against the MAP incidence the model was calibrated against, error bars show the 95% CI's. The vector densities required to produce these estimates were a median of 6.8 (95% CI 3.2 - 35.1).

Impact of *Anopheles stephensi* under different assumptions of populations exposed.

Here we have varied where *An. stephensi* is predicted to increase based on pre-existing estimates of regional suitability for *An. stephensi* as estimated using the geostatistical models of (10). This particularly highlights urban areas, though many people reside in these regions meaning the epidemiological impact could be substantial (Appendix Figure **5**). Another method of generating alternative metrics of the population suitable for ongoing *falciparum* malaria transmission is to only include communities under 2000m, as estimate of an altitude above which malaria transmission is less suitable. This assumption means that a much wider geographical region is suitable but excludes some large cities so the population at risk is substantially lower (

Appendix Table 4).

If *An. stephensi* is confined to areas previously deemed as suitable, then we project an additional 531,000 (134,000 - 979,000) malaria cases a year, and 1,884,000 (542,000 - 3,348,000) if we consider anywhere under 2000m to be suitable. In the most extreme scenario, assuming the entire country is suitable regardless of altitude or prior prediction of suitable, we estimate 3,163,000 (818,000 - 5,740,000) additional malaria cases per year (Appendix Figure 5 and

Appendix Table 4). In all scenarios, these estimates of additional annual malaria cases are substantially larger than the baseline assumption of only areas under 2000m and previously indicated as suitable, of 368,000 (103,000 - 664,000).

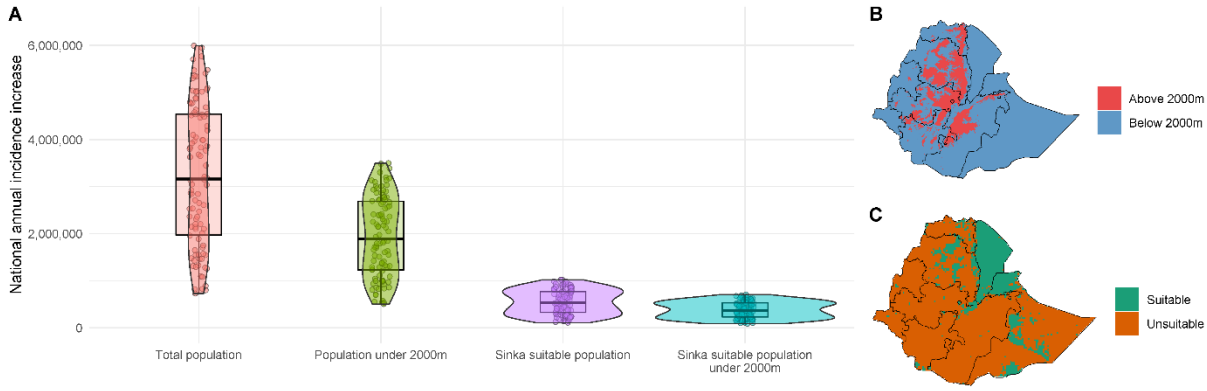

Appendix Figure 5. Sensitivity analyses given uncertainty of the range of environments suitable for *An. stephensi* malaria transmission. A) Comparison of different population denominators on the estimates of increases to malaria incidence, B) Ethiopian areas over/under 2000m altitude and C) Sinka et al., (2020) estimates of suitability of the environment to *An. stephensi* (Sinka suitable in A) normalised to a 0-1 scale, the cut-off assumed was 0.5. Coloured points in panel A, indicate the calculated annual incidence increase for individual LHC runs. Four different situations are considered; (i) – total population where everywhere in Ethiopia is suitable for *An. stephensi* establishment and malaria transmission is possible at altitudes above 2000m, (ii) *An. stephensi* establishment

everywhere but malaria transmission only in areas beneath 2000m altitude, shown in panel B (iii) *An. stephensi* establishes in areas identified by Sinka et al. 2020 to be suitable, shown in panel C, but transmission possible in areas above 2000m, and (iv) areas restricted to those identified by Sinka et al and below 2000m in altitude (matching results shown in main text). Population denominators for the different groupings are shown in Appendix Table 3.

Appendix Table 4. Populations and increase in annual clinical incidence from pre-*An. stephensi* era to after establishment for different scenarios. Sinka suitable denotes areas where the environment has been predicted to be suitable to *An. stephensi* establishment by Sinka et al., (2020).

POPULATION TYPE	POPULATION SIZE	ADDITIONAL CASES (95% CI)
TOTAL POPULATION	114,139,000	3,163,000 (818,000 - 5,740,000)
POPULATION UNDER 2000M	63,564,000	1,884,000 (542,000 - 3,348,000)
SINKA SUITABLE POPULATION UNDER 2000M	12,410,000	368,000 (103,000 - 664,000)
SINKA SUITABLE POPULATION	18,757,000	531,000 (134,000 - 979,000)

Relationship of EIP and increases in prevalence

Areas at higher altitude are predicted to have lower values of temperature dependent EIP (Appendix Figure 7). Following the establishment of *An. stephensi*, there is predicted to be minimal increase in malaria prevalence in areas with high EIPs, those at higher altitudes, compared to those at lower altitudes, and so lower EIPs. This is because the average time for a mosquito to acquire *Plasmodium* infection and then become infectious begins to eclipse the expected lifespan of the mosquito. In these areas even if *An. stephensi* were to establish, it is assumed to have a minimal impact on local malaria transmission.

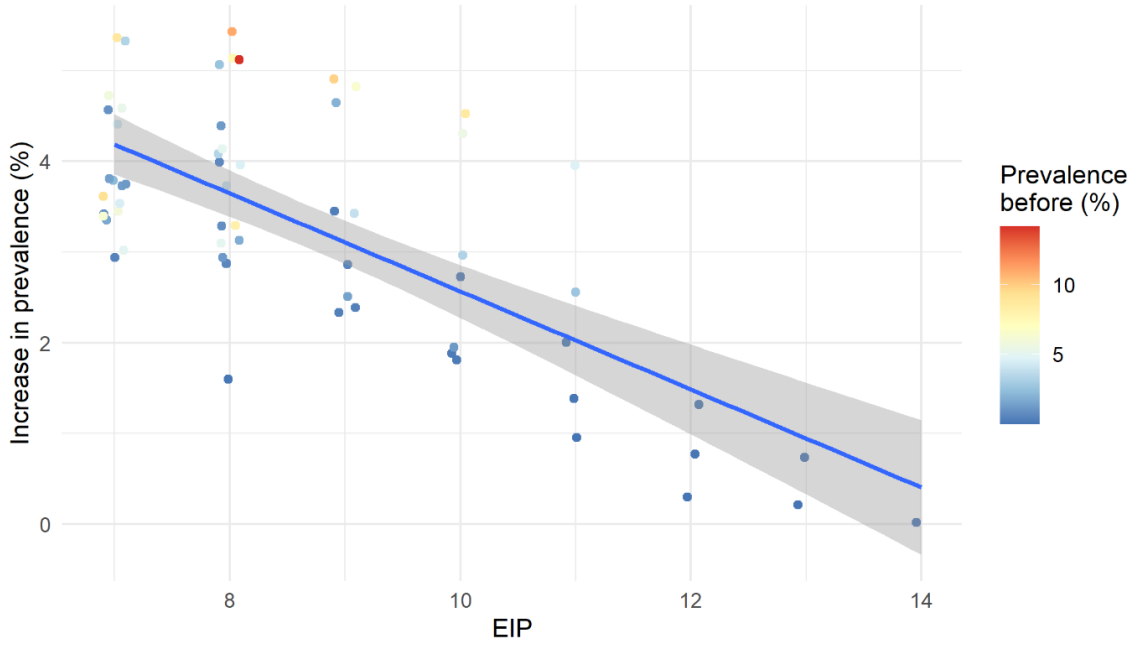

Appendix Figure 6. Relationship of absolute prevalence increase following *An. stephensi* introduction and estimated extrinsic incubation period (EIP) across Ethiopia. Points are jittered on the x-axis to aid interpretation but are integer values in the data. Line represents a linear regression of the relationship of increase in prevalence and EIP. Colour of points refers to the prevalence in all ages pre-*An. stephensi* introduction.

Additional limitations to the modelling approach

Initially mosquito invasion dynamics have been simplified, assuming invasion occurs equally in all locations modelled and that human-to-mosquito densities universally reach the same level as observed in Djibouti. This is unlikely to be the case but is currently the most parsimonious explanation in the absence of other information. Certain locations will be more or less suitable due to local ecological and anthropological conditions, as well as inter-species competition with other mosquito species. This will change both the presence/absence of the species but also their relative abundance. While not accounting for these directly, we have tested the presence/absence assumption by only predicting increases into areas that have been previously estimated to be suitable for *An. stephensi* following an early geostatistical analysis (10) and in those regions under 2000m. While this makes a substantial difference to the overall cases, we still estimate an additional 368,000 (103,000 - 664,000) cases (compared to 3,163,000 (818,000 - 5,740,000) if the whole country is suitable). This different geographical spread will substantially affect the cost of scaling up interventions. Our current model ignores importation of disease through human movement, which could reduce the time between mosquito invasion and increases in disease. Additionally, *An. stephensi* is a highly competent vector for *P. vivax*, found throughout large parts of Ethiopia (17). We have not considered malaria caused by this parasite, and so overall levels of malaria (independent of *Plasmodium* species) are likely to be higher than we have estimated. The model used to quantify the vector density required to explain malaria incidence in Djibouti, and subsequently predict the

potential impact in Ethiopia, is a long standing and extensively tested model against real-world data (1, 3-5, 18, 19). This model was created and utilized in order to model *P. falciparum*, and as such has not been adequately constructed or parameterized for modelling *P. vivax* infection. Due to differences in the progression of disease (primarily relapsing in *P. vivax* malaria due to hypnozoites), predictions of vector density and subsequent impact will therefore be very different between *Plasmodium* species. Noting this, and the greater public health impact of *P. falciparum* infection, we have focused this body of work on *P. falciparum*, while acknowledging this is a limitation in establishing the true potential impact of *An. stephensi*.

The vector may additionally be capable of establishing outside of areas previously predicted to be suitable, and by including the effect of a temperature dependent extrinsic incubation period (EIP), we can partially account for the effect of altitude on malaria transmission. This is shown by many of the regions at higher altitudes, with longer EIPs, have lower increases in prevalence (Appendix Figure **6**). Furthermore, we are not assessing invasion dynamics or timelines, and instead have looked at the differences pre- and post- *An. stephensi* establishment. A more realistic increase in burden would be staggered as establishment will likely vary, which has been seen in *An. stephensi* primarily being detected in eastern and central Ethiopia, so far (17). Finally, we have used a deterministic model structure. The invasion of *An. stephensi* and the subsequent rise of malaria cases is likely to be a highly stochastic process in space and time. This will make predictions of public health impact and the effect of vector control interventions highly uncertain. While mechanistic malaria models have long been used for predicting the impact of interventions in endemic settings (1, 3, 4, 18, 20, 21), this model has not been validated when considering invasion into an area, and so aspects such as the acquisition of immunity in low transmission scenarios should be treated with extreme caution.

This paper has identified a number of different hypotheses such as the speed in the rise of malaria cases will depend on pre-*An.stephensi* malaria endemicity. These hypotheses need to be verified by good quality local surveillance data and models adjusted accordingly.

Future data collection to inform mathematical modelling.

Improved understanding of the current entomological and epidemiological situation in regions where *An. stephensi* may invade will improve projections of its potential public health impact and how effective mitigation measures will be (

Appendix Table 5. Key parameters influencing modelling results and the aspects **of mathematical modelling they inform**. This analysis has highlighted how the increase in malaria burden depends on current malaria endemicity, so more detailed knowledge of the heterogeneity in malaria prevalence and the existing use of vector control interventions in urban and peri-urban areas where the mosquito might invade will be key to understanding overall impact. Malaria burden is also heavily dependent on the abundance of the invading mosquito species and so an understanding of the carrying capacity of the species in the new environment (and how this varies between regions) will enable more tailored projections.

Uncertainty in vector bionomics and behaviours have necessitated several assumptions in this modelling framework. These unknowns, and the sampling structure designed to compensate for them, introduce substantial uncertainty into the results. While a level of uncertainty is expected, with further data on the vector and its role in transmission this can be substantially reduced. Some of the most important vector parameters identified by the model to influence the impact of *An. stephensi* invasion and its control are listed in Table 5 whilst results from a univariate sensitivity analyses showing how mosquito bionomics influence post-An. *stephensi* malaria incidence is given in Appendix Figure 7. We also list the important factors determining intervention effectiveness, many of which will depend on the level of effort deployed. An understanding of the price of these different levels of effort will allow further refinement of the cost-effectiveness analyses.

Appendix Table 5. Key parameters influencing modelling results and the aspects of mathematical modelling they inform.

Parameter type	*Parameter*	*What it informs*
Vector bionomic/ behaviour	Life-expectancy *of An. stephensi* in Africa	Disease endemicity and impact of interventions
	Anthropophagy (human blood index)	Disease endemicity and impact of interventions
	Endophily (mosquito resting behaviour)	Impact of IRS
	Proportion of mosquito bites taken when people indoors	Impact of IRS and ITN
	Proportion of mosquito bites taken when people in bed	Impact of IRS and ITN
	Sporozoite rate in different vector species	Estimate of the relative significance of the invading mosquito population in relation to other local species.
	Seasonality of *An. stephensi* abundance	Impact and requisite frequency of IRS
Intervention Efficacy	Level of pyrethroid resistance	Effectiveness of ITNs (both pyrethroid-only and pyrethroid-PBO nets)
	Percentage of mosquito resting sites accessible to IRS campaigns.	Impact and requisite frequency of IRS
	Durability of IRS in structures in the region (will vary between products)	Impact and requisite frequency of IRS
	Reduction in emergence of adult mosquitoes due to larval source management	Impact of larval source management

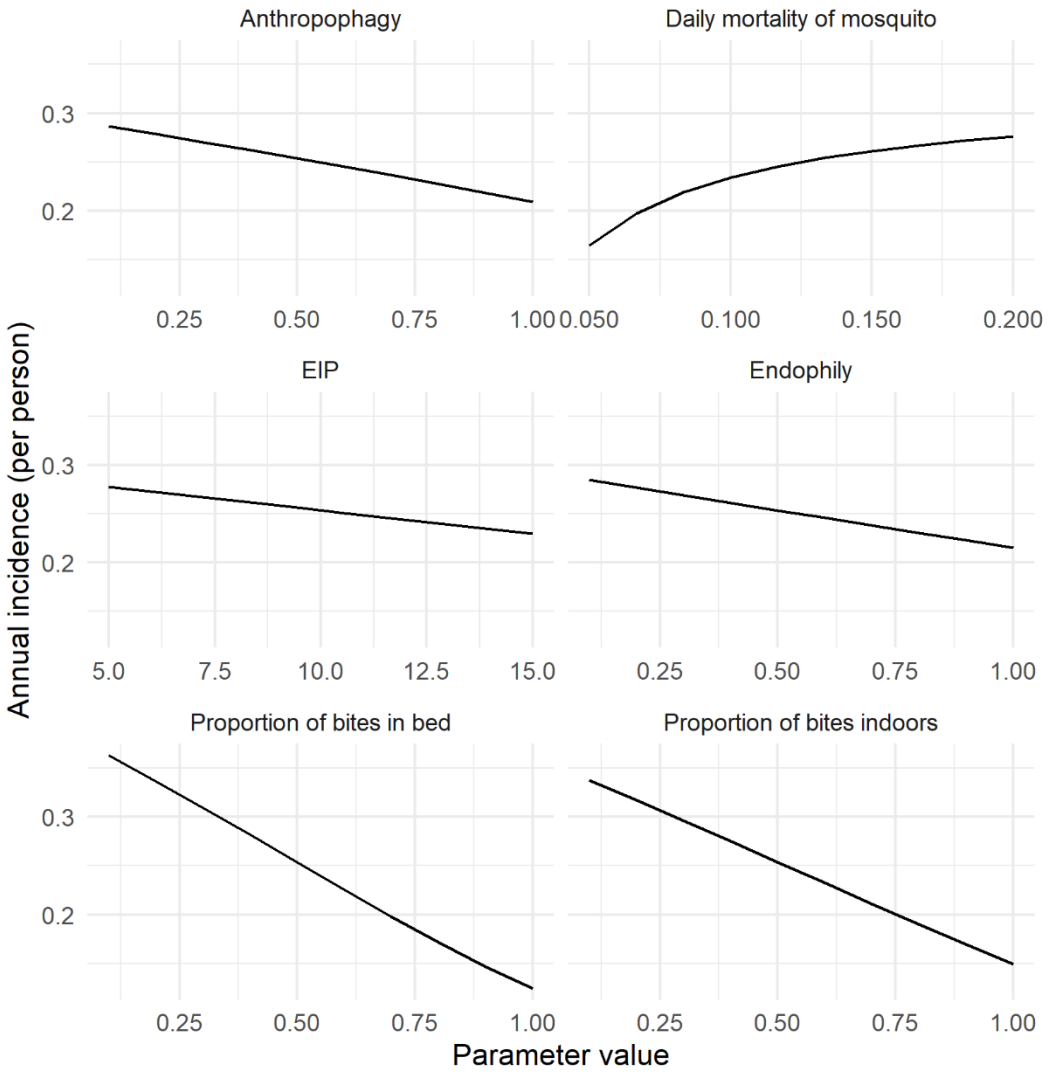

Figure 7. Univariate sensitivity analysis for entomological parameters varied in the model. Results are shown for model predictions of the number of clinical cases per person (per year) in a site with a pre-*An. stephensi* entomological inoculation rate (EIR) of 10 and following the introduction of 50% ITN and IRS coverage after mosquito invasion. EIP is measured in days, the other values are a proportion (0-1).

Appendix Table 6. Vector bionomics taken from literature search.

SOURCE	COUNTRY	URBAN/RURAL	PARAMETER	VALUE
(22)	Iran	rural	proportion of anthropophagy	0.278
(22)	Iran	rural	proportion of anthropophagy	0.183
(22)	Iran	rural	proportion of anthropophagy	0.35
(22)	Iran	rural	proportion of anthropophagy	0.157
(22)	Iran	urban	proportion of anthropophagy	0.435
(23)	Iran	rural	proportion of anthropophagy	0.118
(24)	Iran	rural	proportion of anthropophagy	0.1
(25)	Iran	rural	proportion of anthropophagy	0.27
(25)	Iran	rural	proportion of vector endophily	0.6125
(26)	Iran	rural	endophagy in bed	0.457333333
(27)	India	urban	proportion of vector endophily	0.065408805
(27)	India	urban	proportion of anthropophagy	0.009124088
(28)	Iran	rural	proportion of anthropophagy	0.1983
(29)	India	urban	proportion of anthropophagy	1
(30)	India	unknown	duration of host-seeking behaviour	3
(31)	Iran	rural - mountainous	proportion of vector endophily	0.518
(31)	Iran	rural - plains	proportion of vector endophily	0.538
(32)	Pakistan	rural	proportion of vector endophily	0.80296631
(32)	Pakistan	rural	proportion of vector endophily	0.603058104
(32)	Pakistan	rural	proportion of vector endophily	0.881918819
(33)	Laboratory	NA	daily mortality of adult mosquitoes	0.047619048
(34)	Pakistan	rural	proportion of anthropophagy	0.024
(34)	Pakistan	rural	proportion of anthropophagy	0.016
(34)	Pakistan	rural	daily mortality of adult mosquitoes	0.304878049
(34)	Pakistan	rural	daily mortality of adult mosquitoes	0.266666667
(35)	Kolkata	urban	proportion of vector endophily	0.634408602
(35)	Kolkata	urban	endophagy indoors	0.676

(36)	Laboratory	NA	daily mortality of adult mosquitoes	0.12345679
(37)	India	urban - riverine	proportion of anthropophagy	0.0045
(37)	India	urban - non-riverine	proportion of anthropophagy	0.014
(37)	India	urban	proportion of anthropophagy	0.0103
(37)	Iran	urban	proportion of anthropophagy	0.086
(37)	Iran	urban	proportion of anthropophagy	0.049
(38)	India	urban	proportion of vector endophily	0.214728879
(39)	Iran	rural	proportion of vector endophily	0.38976378
(39)	Iran	rural	proportion of anthropophagy	0.2375
(40)	Ethiopia	rural	proportion of anthropophagy	0.234

Additional References

1. Griffin JT, Ferguson NM, Ghani AC. Estimates of the changing age-burden of *Plasmodium falciparum* malaria disease in sub-Saharan Africa. Nature communications. 2014;5:3136.
2. Challenger JD, Olivera Mesa D, Da DF, Yerbanga RS, Lefèvre T, Cohuet A, et al. Predicting the public health impact of a malaria transmission-blocking vaccine. Nature communications. 2021 2021/03/08;12(1):1494.
3. Griffin JT, Hollingsworth TD, Okell LC, Churcher TS, White M, Hinsley W, et al. Reducing *Plasmodium falciparum* malaria transmission in Africa: a model-based evaluation of intervention strategies. PLoS medicine. 2010 Aug 10;7(8).
4. White MT, Griffin JT, Churcher TS, Ferguson NM, Basanez MG, Ghani AC. Modelling the impact of vector control interventions on *Anopheles gambiae* population dynamics. Parasites & vectors. 2011 Jul 28;4:153.
5. Griffin JT, Bhatt S, Sinka ME, Gething PW, Lynch M, Patouillard E, et al. Potential for reduction of burden and local elimination of malaria by reducing *Plasmodium falciparum* malaria transmission: a mathematical modelling study. Lancet Infect Dis. 2016 Apr;16(4):465-72.
6. Le Menach A, Takala S, McKenzie FE, Perisse A, Harris A, Flahault A, et al. An elaborated feeding cycle model for reductions in vectorial capacity of night-biting mosquitoes by insecticide-treated nets. Malar J. 2007 Jan 25;6:10.
7. Churcher TS, Lissenden N, Griffin JT, Worrall E, Ranson H. The impact of pyrethroid resistance on the efficacy and effectiveness of bednets for malaria control in Africa. Elife. 2016 Aug 22;5.
8. World Population Prospects. https://www.worldpop.org/. [cited 11/01/2021]; Available from:
9. United Nations DoEaSA, Population Division, Population Estimates and Projections Section. World Population Prospects: The 2020 Revision. 2020 [cited; Available from: http://esa.un.org/unpd/wpp/
10. Sinka ME, Pironon S, Massey NC, Longbottom J, Hemingway J, Moyes CL, et al. A new malaria vector in Africa: Predicting the expansion range of *Anopheles stephensi* and identifying the urban populations at risk. Proceedings of the National Academy of Sciences of the United States of America. 2020 Oct 6;117(40):24900-8.
11. Fick SE, Hijmans RJ. WorldClim 2: new 1-km spatial resolution climate surfaces for global land areas. Int J Climatol. 2017 Oct;37(12):4302-15.
12. Stopard IJ, Churcher TS, Lambert B. Estimating the extrinsic incubation period of malaria using a mechanistic model of sporogony. Plos Comput Biol. 2021 Feb;17(2):e1008658.
13. Shapiro LLM, Whitehead SA, Thomas MB. Quantifying the effects of temperature on mosquito and parasite traits that determine the transmission potential of human malaria. PLoS Biol. 2017 Oct;15(10):e2003489.
14. Shapiro LL, Murdock CC, Jacobs GR, Thomas RJ, Thomas MB. Larval food quantity affects the capacity of adult mosquitoes to transmit human malaria. Proc Biol Sci. 2016 Jul 13;283(1834).
15. Murdock CC, Sternberg ED, Thomas MB. Malaria transmission potential could be reduced with current and future climate change. Sci Rep. 2016 Jun 21;6:27771.
16. Bompard A, Da DF, Yerbanga SR, Morlais I, Awono-Ambene PH, Dabire RK, et al. High *Plasmodium infection* intensity in naturally infected malaria vectors in Africa. Int J Parasitol. 2020 Oct;50(12):985-96.
17. Tadesse FG, Ashine T, Teka H, Esayas E, Messenger LA, Chali W, et al. Anopheles stephensi Mosquitoes as Vectors of *Plasmodium vivax* and *falciparum*, Horn of Africa, 2019. Emerging infectious diseases. 2021 Feb;27(2):603-7.
18. Griffin JT. The Interaction between Seasonality and Pulsed Interventions against Malaria in Their Effects on the Reproduction Number. Plos Comput Biol. 2015 Jan;11(1).

19. Walker PG, Griffin JT, Ferguson NM, Ghani AC. Estimating the most efficient allocation of interventions to achieve reductions in *Plasmodium falciparum* malaria burden and transmission in Africa: a modelling study. Lancet Glob Health. 2016 Jul;4(7):e474-84.
20. Walker TM, Lalor MK, Broda A, Ortega LS, Morgan M, Parker L, et al. Assessment of *Mycobacterium tuberculosis* transmission in Oxfordshire, UK, 2007-12, with whole pathogen genome sequences: an observational study. Lancet Resp Med. 2014 Apr;2(4):285-92.
21. Cairns ME, Walker PG, Okell LC, Griffin JT, Garske T, Asante KP, et al. Seasonality in malaria transmission: implications for case-management with long-acting artemisinin combination therapy in sub-Saharan Africa. Malar J. 2015 Aug 19;14:321.
22. Manouchehri AV, Javadian E, Eshighy N, Motabar M. Ecology of *Anopheles stephensi* Liston in southern Iran. Trop Geogr Med. 1976 Sep;28(3):228-32.
23. Mehravaran A, Vatandoost H, Oshaghi MA, Abai MR, Edalat H, Javadian E, et al. Ecology of *Anopheles stephensi* in a malarious area, southeast of Iran. Acta Med Iran. 2012;50(1):61-5.
24. Vatandoost H, Oshaghi MA, Abaie MR, Shahi M, Yaaghoobi F, Baghaii M, et al. Bionomics of *Anopheles stephensi* Liston in the malarious area of Hormozgan province, southern Iran, 2002. Acta tropica. 2006 Feb;97(2):196-203.
25. Mojahedi AR, Safari R, Yarian M, Pakari A, Raeisi A, Edalat H, et al. Biting and resting behaviour of malaria vectors in Bandar-Abbas County, Islamic Republic of Iran. East Mediterr Health J. 2020 Oct 13;26(10):1218-26.
26. Basseri HR, Abai MR, Raeisi A, Shahandeh K. Community sleeping pattern and anopheline biting in southeastern Iran: a country earmarked for malaria elimination. The American journal of tropical medicine and hygiene. 2012 Sep;87(3):499-503.
27. Thomas S, Ravishankaran S, Justin NA, Asokan A, Mathai MT, Valecha N, et al. Resting and feeding preferences of *Anopheles stephensi* in an urban setting, perennial for malaria. Malar J. 2017 Mar 10;16(1):111.
28. Basseri H, Raeisi A, Ranjbar Khakha M, Pakarai A, Abdolghafar H. Seasonal abundance and host-feeding patterns of anopheline vectors in malaria endemic area of iran. J Parasitol Res. 2010;2010:671291.
29. Dash AP, Adak T, Raghavendra K, Singh OP. The biology and control of malaria vectors in India. Curr Sci. 2007;92(11):1571-8.
30. Conn JE, Norris DE, Donnelly MJ, Beebe NW, Burkot TR, Coulibaly MB, et al. Entomological Monitoring and Evaluation: Diverse Transmission Settings of ICEMR Projects Will Require Local and Regional Malaria Elimination Strategies. The American Journal of Tropical Medicine and Hygiene. 2015 Sep;93(3 Suppl):28-41.
31. Maghsoodi N, Ladonni H, Basseri HR. Species Composition and Seasonal Activities of Malaria Vectors in an Area at Reintroduction Prevention Stage, Khuzestan, South-Western Iran. J Arthropod Borne Dis. 2015 Jun;9(1):60-70.
32. Herrel N, Amerasinghe FP, Ensink J, Mukhtar M, van der Hoek W, Konradsen F. Adult anopheline ecology and malaria transmission in irrigated areas of South Punjab, Pakistan. Medical and Veterinary Entomology. 2004 Jun;18(2):141-52.
33. O'Donnell AJ, Rund SSC, Reece SE. Time-of-day of blood-feeding: effects on mosquito life history and malaria transmission. Parasites & Vectors. 2019 2019/07/02;12(1):301.
34. Reisen WK, Boreham PF. Estimates of malaria vectorial capacity for *Anopheles culicifacies* and *Anopheles stephensi* in rural Punjab province Pakistan. J Med Entomol. 1982 Jan 28;19(1):98-103.
35. Ghosh A, Mandal S, Chandra G. Seasonal distribution, parity, resting, host-seeking behavior and association of malarial parasites of *Anopheles stephensi* Liston in Kolkata, West Bengal. Entomological Research. 2010;40(1):46-54.
36. Reisen WK, Mahmood F. Horizontal Life Table Characteristics of the Malaria Vectors *Anopheles culicifacies* and *Anopheles stephensi* (Diptera: Culicidae)1. J Med Entomol. 1980;17(3):211-7.

37. Sinka ME, Bangs MJ, Manguin S, Chareonviriyaphap T, Patil AP, Temperley WH, et al. The dominant *Anopheles* vectors of human malaria in the Asia-Pacific region: occurrence data, distribution maps and bionomic precis. Parasites & Vectors. 2011 May 25;4:89.
38. Pramanik MK, Aditya G, Raut SK. A survey of anopheline mosquitoes and malarial parasite in commuters in a rural and an urban area in West Bengal, India. J Vector Borne Dis. 2006 Dec;43(4):198-202.
39. Soleimani-Ahmadi M, Vatandoost H, Shaeghi M, Raeisi A, Abedi F, Eshraghian MR, et al. Field evaluation of permethrin long-lasting insecticide treated nets (Olyset®) for malaria control in an endemic area, southeast of Iran. Acta tropica. 2012 Sep;123(3):146-53.
40. Ashine T, Teka H, Esayas E, Messenger LA, Chali W, Meerstein-Kessel L, et al. *Anopheles stephensi* as an emerging malaria vector in the Horn of Africa with high susceptibility to Ethiopian *Plasmodium vivax* and *Plasmodium falciparum* isolates. bioRxiv. 2020:2020.02.22.961284.